

Fig. 3. Plan view (computer-drawn) of the basalt platform with two walls, with superimposed magnetic anomaly contours (in gammas). Blocks 1, 2, and 3 come to within 1.0, 1.0, and 1.5 m of the pyramid's surface, respectively. Block 1: $Z = 20.75$; $\Delta z = 0.25$. Block 2: $Z = 21.50$; $\Delta z = 0.50$. Block 3: $Z = 22.50$; $\Delta z = 1.50$. The point 0,0,30 is located at the center of the pyramid and 30 m above its base.

suming a "normal basalt," it is evident that the choice of 10^{-3} is probably conservative. It has also been assumed that the magnetization is uniform and is in the direction of the earth's field.

The values of the model anomaly have been calculated for points on the surface of an equivalent cone; these project in plan to an equidimensional grid. These points are then contoured within the computer program, and the resulting anomaly is plotted by a Calcomp plotter and compared with the field data.

Tests of models representing discontinuities in the soil layer (that is, pits) indicated that the anomaly could also be produced by some slablike body at least 4 m thick with a susceptibility of approximately 10^{-4} . There are several possible forms that this structure could take. One would be a pit filled with highly organic soil. Another would be a pit filled with some stone other than basalt. It is difficult to imagine that a pit of this composition and dimension would show no erosional expression and no surface geological expression. Should the pit contain a less susceptible stone than basalt (for instance, serpentine), then a significant archeological structure would still be indicated.

The fitting of "standard" buried block models is a matter of trial and error procedures. This process is extremely tedious and is quite costly in computer time; therefore, the present analysis has not been continued be-

yond a model that provides a basic fit. The final multiple block model that was found to provide a good basic fit to the data consists of a thin 10- by 10-m platform with peripheral walls on the northern and eastern sides (see dotted outline in Fig. 3). The horizontal location to the center of mass of the block is given in this plan drawing, with the vertical coordinate (Z) to its center and the half-height (Δz) given in the figure legend. The x coordinate is positive north, y is positive east, and z is positive up, all with respect to the base and center of the pyramid. The enclosing margin of the model location plot and the resulting model anomaly (Fig. 3) correspond to the inner rectangle of Fig. 2.

The calculated anomaly (Fig. 3) fits the field data surprisingly well, except that the background level of these theoretical data must be raised over a broad area and its western side must be stretched out. It appears that an even deeper structure is responsible for this broadening in the field data. The effects of topography and the generally disturbed area within 4 m of the top all combine to complicate the interpretation. However, it may be safely concluded from this model work that the basalt structure comes within 1 to 2 m of the surface and is of the general form suggested by the slab-plus-walls model.

FRANK MORRISON
JOSÉ BENAVENTE

Department of Materials Science
and Engineering, University of
California, Berkeley 94720

C. W. CLEWLOW, JR.
R. F. HEIZER

Department of Anthropology,
University of California

References and Notes

1. M. W. Stirling, *Bur. Amer. Ethnol. Bull.* **138** (1943); P. Drucker, *ibid.* **153** (1952).
2. P. Drucker, R. F. Heizer, R. J. Squier, *ibid.* **170** (1955); P. Drucker and R. F. Heizer, *Kroeber Anthropol. Soc. Pap.* **33**, 37 (1965).
3. R. F. Heizer and P. Drucker, *Antiquity* **42**, 75 (1968).
4. R. F. Heizer, in *Dumbarton Oaks Conference on the Olmec*, E. Benson, Ed. (Dumbarton Oaks, Washington, D.C., 1968), pp. 9-40.
5. ———, P. Drucker, J. A. Graham, *Inst. Nac. Antropol. Hist. Bol.* **33**, 21 (1968).
6. R. F. Heizer, J. A. Graham, L. K. Napton, *Contrib. Univ. Calif. Archaeol. Res. Facil.* **5** (1968), pp. 127-154.
7. M. D. Coe, *America's First Civilization: Discovering the Olmec* (American Heritage, New York, 1968), p. 56.
8. I. Bernal, *The Olmec World* (Univ. of California Press, Berkeley, 1969), pp. 35-36.
9. H. Williams and R. F. Heizer, *Contrib. Univ. Calif. Archaeol. Res. Facil.* **1** (1965), pp. 1-39.
10. S. Breiner, *Science* **150**, 185 (1965); F. Rainey and E. K. Ralph, *ibid.* **153**, 1481 (1966); E. K. Ralph, F. Morrison, D. P. O'Brien, *Geoscientific* **8**, 109 (June 1968).

11. E. Le Borgne, *Ann. Geophys.* **11**, 399 (1955); M. J. Aitken, *Physics and Archaeology* (Interscience, New York, 1961); J. C. Cook and S. L. Carts, *J. Geophys. Res.* **67**, 815 (1962).
12. B. K. Bhattacharyya, *Geophysics* **29**, 517 (1964).
13. Supported by the National Geographic Society Committee on Research and Exploration. We thank Professor J. Barcus, University of Denver, for the loan of one of the magnetometers; Dr. Ignacio Bernal, Director of the Instituto Nacional de Antropología e Historia (Mexico), for the necessary permits; Señor Paul Quiros of INAH for assistance with customs; and Arql. Eduardo Contreras and Arql. Carlos Sebastian Hernandez for assistance in the field. The Computer Center of the Berkeley campus provided the computer time for the model studies.

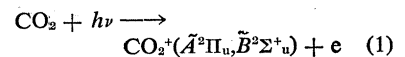
4 December 1969; revised 19 January 1970

Mariner 6: Origin of Mars Ionized Carbon Dioxide Ultraviolet Spectrum

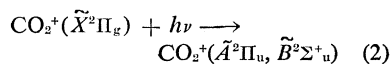
Abstract. *The predicted intensities of the ionized carbon dioxide (CO_2^+) emission feature at 2890 angstroms and the Fox-Duffendack-Barker bands are 5.2 and 19.9 kilorayleighs, respectively, for a vertical column. Direct photo-ionization of carbon dioxide by solar radiation contributes 3.5 and 4.1 kilorayleighs, respectively, and fluorescent scattering by CO_2^+ , 1.6 and 15.3 kilorayleighs, respectively. Photoelectron impacts are less important.*

Studies by Barth *et al.* of Mariner 6 spectra (1) have established that the Fox-Duffendack-Barker bands and the CO_2^+ ultraviolet doublet bands are important components of the dayglow of Mars. Barth *et al.* (1) noted that the Mars spectrum they observed is similar to that produced in the laboratory by the bombardment of CO_2 by 20-ev electrons, and they pointed out that the excitation mechanisms that occur on Mars may or may not be electron-impact processes. Our calculations show that most of the excitations arise from photo-ionization of CO_2 and fluorescent scattering by CO_2^+ and that comparatively few excitations arise from electron impacts.

The Fox-Duffendack-Barker band system corresponds to the transition from the $\tilde{A}^2\Pi_u$ state to the $\tilde{X}^2\Pi_g$ state that emits over a broad region between 3000 and 4500 Å, and the CO_2^+ ultraviolet doublet band system corresponds to the transition from the $\tilde{B}^2\Sigma^+_u$ state to the $\tilde{X}^2\Pi_g$ state that emits over a narrow region near 2890 Å. The excited $\tilde{A}^2\Pi_u$ and $\tilde{B}^2\Sigma^+_u$ levels of CO_2^+ can be populated (i) by direct photo-ionization of CO_2 by solar radiation



(ii) by fluorescent scattering of solar radiation by preexisting CO_2^+ ions



and (iii) by simultaneous excitation and ionization of CO_2 by photoelectron impact



If we assume that the neutral component of the atmosphere of Mars is effectively pure CO_2 , the total rates of population of the electronic levels of CO_2^+ by photo-ionization can be estimated directly from the cross-section data at 584 Å (2) and the incident solar flux. The resulting rates of production of the $\tilde{A}^2\Pi_u$ and $\tilde{B}^2\Sigma^+_u$ states of CO_2 in a vertical column are, respectively, $3.4 \times 10^9 \text{ cm}^{-2} \text{ sec}^{-1}$ and $3.3 \times 10^9 \text{ cm}^{-2} \text{ sec}^{-1}$ for the solar zenith angle of 27° , appropriate to the Mariner 6 observations. If no deactivation or cascading occurred, the rates of population would also be the emission intensities. Deactivation is negligible, radiative lifetimes being about 10^{-7} second (3), but the $\tilde{C}^2\Sigma^+_g$ state of CO_2^+ decays to both $\tilde{A}^2\Pi_u$ and $\tilde{B}^2\Sigma^+_u$ states. We assume arbitrarily that the branching ratio is 4 : 1. The predicted intensities of the two emission systems in kilorayleighs are given in Table 1.

As described by Chamberlain (4), the fluorescent scattering efficiencies g for the two systems may be calculated from the laboratory lifetime data (3). We obtain for a zenith angle of 0° $g = 1.1 \times 10^{-2}$ for the $\tilde{A}^2\Pi_u$ state and $g = 1.2 \times 10^{-3}$ for the $\tilde{B}^2\Sigma^+_u$ state. If we assume that the ionic component of Mars is pure CO_2^+ , the fluorescent intensities can be derived from data on the total electron content. The total electron content derived from Mariner 6 occultation data (5) at a solar zenith angle of 56° was $1.1 \times 10^{12} \text{ cm}^{-2}$. A linear scaling procedure based upon an ionization balance be-

tween photo-ionization and dissociative recombination leads to a total electron content of $1.4 \times 10^{12} \text{ cm}^{-2}$ at 27° . The corresponding fluorescent intensities are given in Table 1.

The energy flux of photoelectrons with sufficient energy to simultaneously excite and ionize CO_2 is about $3 \times 10^{11} \text{ ev cm}^{-2} \text{ sec}^{-1}$ on Mars. Detailed calculations of the energy degradation of photoelectrons in a pure CO_2 atmosphere, which are similar to calculations carried out for photoelectrons in air (6), yield the intensities given in Table 1.

Table 1 compares the contributions from the three sources. Photo-ionization is the strongest source of the ultraviolet bands at 2890 Å, and fluorescent scattering is the strongest source of the Fox-Duffendack-Barker band system. Photoelectron impact contributes not more than 5 percent for either transition.

Our conclusion that electron impact excitations are unimportant is unlikely to be altered by modifications in the adopted neutral and ionic composition or in the laboratory cross-section data. Data on the actual intensities observed from Mariner 6 would be of great in-

terest. Similar predictions for Venus at a solar zenith angle of 27° , based upon Mariner 5 data, are also included in Table 1.

A. DALGARNO

Harvard College Observatory and
Smithsonian Astrophysical Observatory,
Cambridge, Massachusetts 02138

T. C. DEGGES

Technology Division, GCA Corporation,
Bedford, Massachusetts 01730

A. I. STEWART

Laboratory for Atmospheric and
Space Physics, University of
Colorado, Boulder 80302

References

1. C. A. Barth, W. G. Fastie, C. W. Hord, J. B. Pearce, K. K. Kelly, A. I. Stewart, G. E. Thomas, G. P. Anderson, O. F. Raper, *Science* **165**, 1004 (1969).
2. J. L. Bahr, A. J. Blake, J. H. Carver, V. Kumar, *J. Quant. Spectros. Radiat. Transfer* **9**, 1359 (1969); D. W. Turner and D. P. May, *J. Chem. Phys.* **45**, 471 (1966); R. Spöhr and E. von Puttkamer, *Z. Naturforsch.* **22a**, 705 (1967).
3. J. E. Hesser, *J. Chem. Phys.* **48**, 2518 (1968).
4. J. W. Chamberlain, *Physics of the Aurora and Airglow* (Academic Press, New York, 1961).
5. G. Fjeldbo, A. Kliore, B. Seidel, *Radio Sci.*, in press.
6. A. E. S. Green and C. A. Barth, *J. Geophys. Res.* **72**, 3975 (1967); A. Dalgarno, M. B. McElroy, A. I. Stewart, *J. Atmos. Sci.* **26**, 753 (1969).

1 December 1969; revised 12 January 1970 ■

Viscosity of Lunar Lavas

Abstract. *The viscosity of a synthetic silicate liquid with the composition of a lunar rock has been determined experimentally and found to be lower than that of any previously studied volcanic rock on earth. This fact suggests that lunar lava flows will be very thin and extensive unless they are ponded, and that lava tubes should be common and of larger dimensions than those on earth. Coarse crystallinity can be a feature of rapidly cooled surface lavas.*

Perhaps the most startling characteristics of the lunar samples returned from the Apollo 11 mission are their high contents of iron and titania, which exceed those of any known terrestrial volcanic rocks. The coarsely crystalline nature of many of the rocks suggests that the unusual composition was responsible for the low viscosity and for the ability of the rocks to flow and vesiculate but still to grow crystals of large dimension at the surface or at shallow depths where cooling is relatively rapid.

In order to investigate this possibility, we have determined the viscosity of a synthetic silicate liquid of lunar composition over a range of temperature above its liquidus. A 200-g sample was prepared with the same composition (in percentage by weight), except for the last two components listed, as that given for specimen 22 in the report of the

preliminary examination team of the Apollo 11 samples (1): SiO_2 , 43; TiO_2 , 11; Al_2O_3 , 7.7; FeO , 21; MnO , 0.26; MgO , 6.5; CaO , 9.0; Na_2O , 0.40; K_2O , 0.21; Cr_2O_3 , 0.41; ZrO_2 , 0.14; and NiO , 0.04. A solution was prepared of nitrates of Al, Fe, Mg, Ca, Na, K, Mn, and Cr in a mixture of ethanol and water. To this a weighed quantity of tetraethyl orthosilicate was added, and a gel was precipitated by the addition of ammonia. Water and NO_2 were then driven off by slowly heating the sample at successively higher temperatures. Titanium dioxide was added and ground together with the sintered material, and then the combined sample was heated to fusion at a maximum temperature of 1500°C .

On the basis of observations of the crystallization of samples cooled from temperatures between 1250° and 1500°C we believe that the liquidus temperature

Table 1. Predicted intensities (in kilorayleighs) of the $\tilde{X}^2\Pi_g$ - $\tilde{A}^2\Pi_u$ and $\tilde{X}^2\Pi_g$ - $\tilde{B}^2\Sigma^+_u$ band systems of CO_2^+ on Mars and Venus at a solar zenith angle of 27° .

System	Mars		Venus	
	$\tilde{A}^2\Pi_u$	$\tilde{B}^2\Sigma^+_u$	$\tilde{A}^2\Pi_u$	$\tilde{B}^2\Sigma^+_u$
Photo-ionization	4.1	3.5	17.5	15.0
Fluorescent scattering	15.3	1.6	82.6	8.4
Photoelectron impact	0.5	0.1	2.2	0.6
Total	19.9	5.2	102.3	24.0